

# Triplet NOAH supersequences optimised for small molecule structure characterisation

Tim D. W. Claridge,<sup>1</sup> Maksim Mayzel,<sup>2</sup> and Ēriks Kupče<sup>3</sup>

- 1) Department of Chemistry, University of Oxford, Chemistry Research Laboratory, Mansfield Road, Oxford, OX1 3TA, UK.
- 2) Bruker BioSpin AG, Industriestrasse 26, 8117 Fällanden, Switzerland
- 3) Bruker UK Ltd., Banner Lane, Coventry, CV4 9GH, UK

## Keywords

NMR; NOAH; MFA; HMBC; HSQC; COSY; TOCSY; NOESY; ROESY; NUS

## Abstract

A series of NMR supersequences are presented for the time-efficient structure characterisation of small molecules in the solution state. These triplet sequences provide HMBC, HSQC and one homonuclear correlation experiment of choice according to the NOAH (NMR by Ordered Acquisition using  $^1\text{H}$  detection) principle. The experiments are demonstrated to be compatible with non-uniform sampling (NUS) schemes and may be acquired and processed under full automation.

## Introduction

The structure characterisation of small organic molecules typically involves the collection of a set of 2D NMR experiments that are combined to elucidate the core atom connectivity within the molecule and thereby define its primary structure. These rely routinely on a series of homonuclear  $^1\text{H}$ - $^1\text{H}$  and heteronuclear  $^1\text{H}$ - $^{13}\text{C}$  correlation experiments. Subsequent investigations may employ homonuclear methods that exploit through-space (dipolar) proton interactions to define the configuration (stereochemistry) and/or conformation of the molecule. Traditionally such experiments are collected as a series of individual 2D data sets, the time requirements for each defined by the fundamental requirements of sensitivity (number of transients collected) and resolution (number of increments employed), but also by the need to allow sufficient time between acquired transients for nuclear magnetisation to relax toward the equilibrium state. This period, the relaxation or recovery delay, is typically the longest element of any pulse sequence and represents time in which the NMR instrument is passive and, in effect, unemployed. In recent work we have demonstrated the possibility of concatenating a series of 2D sequences such that only a single recovery delay is employed in a single “supersequence” which ultimately produces a nest of 2D experiments that may be employed for structure characterisation.<sup>1, 2</sup> This leads to significant time-savings in data

collection, optimising use of valuable instrument time and reducing instrument redundancy. The approach relies on the appropriate ordering of individual techniques (modules) within each supersequence to control the sequential sampling of magnetisation pools, thus yielding the required data sets for characterisation in an approach that has been termed NOAH- *NMR by Ordered Acquisition using  $^1\text{H}$  detection*. The NOAH approach represents one category of techniques that employ multi-FID acquisitions in a single concatenated experiment which are gaining recognition as time-efficient data collection strategies.<sup>3-6</sup> These are attractive as they can be executed using conventional spectrometer hardware without the need for multiple receivers, as used in parallel acquisition NMR spectroscopy (PANSY),<sup>7-9</sup> nor do they suffer the technical complexities associated with single-scan ultrafast correlation methods.<sup>10-12</sup>

Recently we have demonstrated the NOAH BS- element as being the optimum ordering to sample HMBC (B) and HSQC (S) correlation data in a single experiment and exemplified its use in the BSC and BSCN combinations (where C signifies COSY and N NOESY).<sup>2</sup> The sequence was designed to sample long-range  $^1\text{H}$ - $^{13}\text{C}$  correlations (arising from  $^n\text{J}_{\text{CH}}$  couplings, where  $n = 2$  or  $3$ ) in the initial ZZ-HMBC module whilst leaving  $^1\text{J}_{\text{CH}}$  magnetisation along the z-axis ready for sampling in the subsequent HSQC module. Herein we demonstrate the versatility of the “BS-” parent combination by presenting a series of NOAH triplet experiments that combine HMBC and HSQC with an additional homonuclear 2D correlation of choice. These experiments are suitable for the time-efficient, routine characterisation of small molecules under automated environments, especially those arising from synthetic chemistry programs.

## Results and Discussion

The new methods develop from the previously introduced NOAH-3 BSC that comprises the ZZ-HMBC-HSQC-ASAP-COSY sequence. Briefly, this provides for conventional HMBC, multiplicity-edited HSQC and 2D COSY (that optionally employs a brief ASAP isotopic mixing period prior to the COSY data acquisition to distribute longitudinal magnetisation more evenly amongst coupled protons<sup>13, 14</sup>). The COSY experiment may be collected without  $F_1$  quadrature detection, thus matching the widely used “magnitude mode” COSY experiment, but equally may be acquired with phase-sensitive  $F_1$  detection. Furthermore, as this homonuclear module utilises recovered longitudinal  $^1\text{H}$  z-magnetisation as its source, it provides the possibility of replacing the COSY module with any (phase-sensitive) homonuclear correlation “X”, yielding multiple NOAH-3 BSX combinations. Some attractive options for the routine characterisation of small molecules are presented in Figure 1. These incorporate the commonly employed 2D homonuclear correlation elements such as TOCSY, NOESY and ROESY, but also the recently

proposed CLIP-COSY (clean in-phase COSY)<sup>15</sup> that provides for high-resolution phase-sensitive COSY presentation and the classic double-quantum filtered COSY (DQF-COSY).

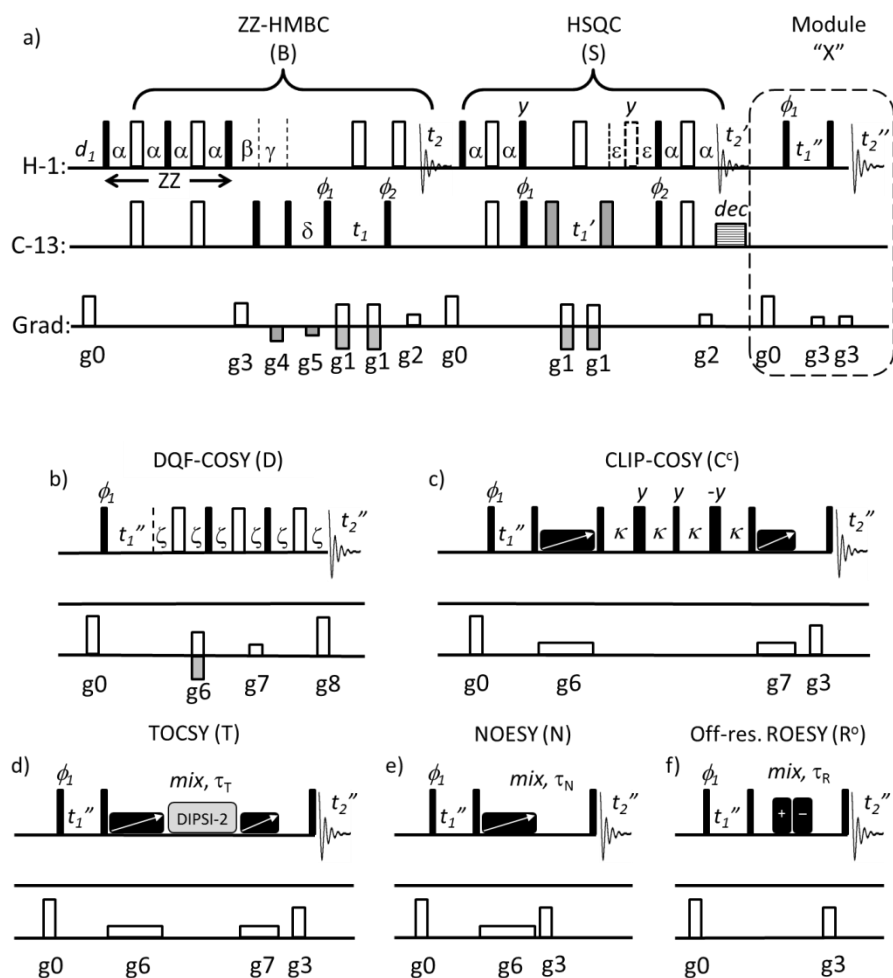


**Figure 1:** The family of NOAH-3 BSX experiments for which X represents a phase-sensitive homonuclear correlation. a) Representation of the parent BSX sequence providing HMBC (B) and HSQC (S) spectra, with X as the standard magnitude mode COSY (C) experiment (shown without optional ASAP mixing element) and (b-f) alternative homonuclear "X" modules yielding b) DQF-COSY (D), c) CLIP-COSY (C<sup>c</sup>), d) TOCSY (T), e) NOESY (N), and f) ROESY (R) spectra. The filled bars represent 90° pulses and the open bars 180° pulses; the dotted 180° bar in the HSQC module signifies optional multiplicity editing and the greyed 180° HSQC pulses represent the associated J-compensated adiabatic sweeps. Delays  $\alpha = 1/4 \cdot J_{CH}$ ,  $\beta = 1/2 \cdot J_{CH}(\min)$ ,  $\gamma = 1/2 \cdot J_{CH}(\max)$ ,  $\delta = 1/2 \cdot J_{CH}$ ,  $\varepsilon = 1/2 \cdot J_{CH}$ ,  $\zeta =$  gradient pulse duration plus recovery delay,  $\kappa = 1/4 \cdot J_{HH}$  and  $\tau_X$  represents the mixing time for each module, where employed. Delays  $\beta$  and  $\gamma$  serve as low-pass filters in the HMBC module. In all cases  $g_0$  represents a purging gradient of arbitrary intensity to select longitudinal <sup>1</sup>H magnetisation. Gradients  $g_1$  and  $g_2$  provide coherence selection with  $g_1 = 2 \cdot g_2$ . Echo-anti-echo selection is employed for HMBC and HSQC via alternation of  $g_2$ , and for DQF-COSY through alternating  $g_6$ . The remaining homonuclear experiments employ either States or States-TPPI detection. In modules (c) to (f),  $g_3$  is a purging gradient, with  $g_6$  and  $g_7$  employed in zero-quantum suppression elements in modules (c) to (e) for which the arrowed, filled rectangles represent frequency-swept adiabatic pulses. The TOCSY module makes use of the DIPSI-2 mixing sequence and the off-resonance ROESY (R<sup>0</sup>) employs a pair of adiabatic pulses indicated by the filled rectangles with high (+) then low (-) frequency offsets. All pulses are applied with phase x unless indicated otherwise and follow  $\phi_1 = x, -x$ ;  $\phi_2 = x, x, -x, -x$ ;  $rec = x, -x, -x, x$ . For States-based sampling, additional phase-cycling of the <sup>1</sup>H initial excitation pulse is employed on incrementing  $t_1''$  in modules (c) to (f).

As shown in Fig 1, the HMBC module is implemented using a two-step low-pass filter which, together with the ZZ-preparation element, leads to efficient suppression of unwanted one-bond correlations. The optional HSQC multiplicity editing element benefits from utilising J-compensated adiabatic  $^{13}\text{C}$  pulses for cleaner editing.<sup>16, 17</sup> The homonuclear elements incorporate the usual desirable refinements including zero-quantum filtration<sup>18</sup> in the CLIP-COSY, TOCSY and NOESY variants. The ROESY experiment employs a pair of off-resonance adiabatic pulses in a manner similar to that proposed in the EASY-ROESY<sup>19</sup> method, for which the sum of the off-resonance spinlock pulse durations defines the total ROE mixing period. Alternatively, the mixing may be achieved using a repeating pair of phase-alternating  $180^\circ$  hard pulses as in the transverse-ROESY<sup>20</sup> method (SI Fig S3), although we find the adiabatic mixing typically provides slightly greater efficiency.

The performance of the BSX family and the quality of data produced are demonstrated with the diterpene andrographolide. The HMBC and edited-HSQC spectra are shown for the BSC<sup>c</sup> experiment (Fig 2) but appear similar for all BSX variants, as expected. Spectra for each of the homonuclear elements from separate NOAH experiments show the anticipated cross peak structures (Fig 3) with data quality at least comparable to that of the conventional single homonuclear experiments (SI fig S1). In the case of DQF COSY, the NOAH data demonstrated a marked reduction in rapid-pulsing artefacts that are commonly observed in the conventional experiment. For the andrographolide sample, ROESY spectra exhibited significantly greater crosspeak intensity than NOESY at 700 MHz due to the combination of molecular correlation time and field strength employed, whereas the spectra were of more comparable intensity at 500 MHz (SI fig S2).

The time savings offered by the NOAH approach are exemplified by the time requirements for each NOAH acquisition versus that of the total time for the three individually recorded data sets collected with identical resolution and number of transients (Fig 3, Table 1 and SI Table S1). In all cases the NOAH approach leads to in excess of a two-fold time saving.

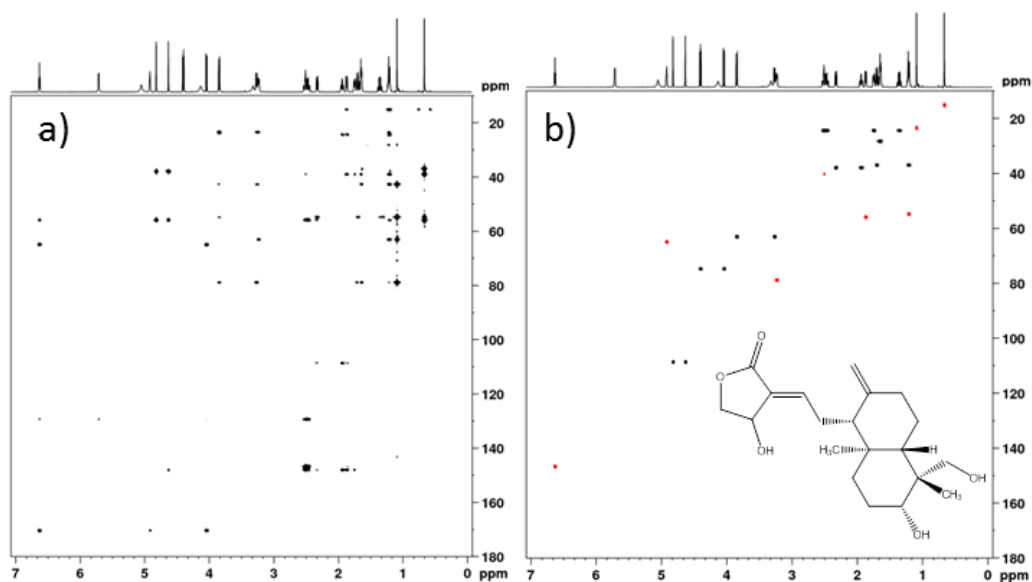


**Figure 2:** The a) HMBC and b) multiplicity-edited HSQC spectra recorded in the NOAH-3 BSC experiment performed on andrographolide (38 mM, DMSO). See Experimental section for details.

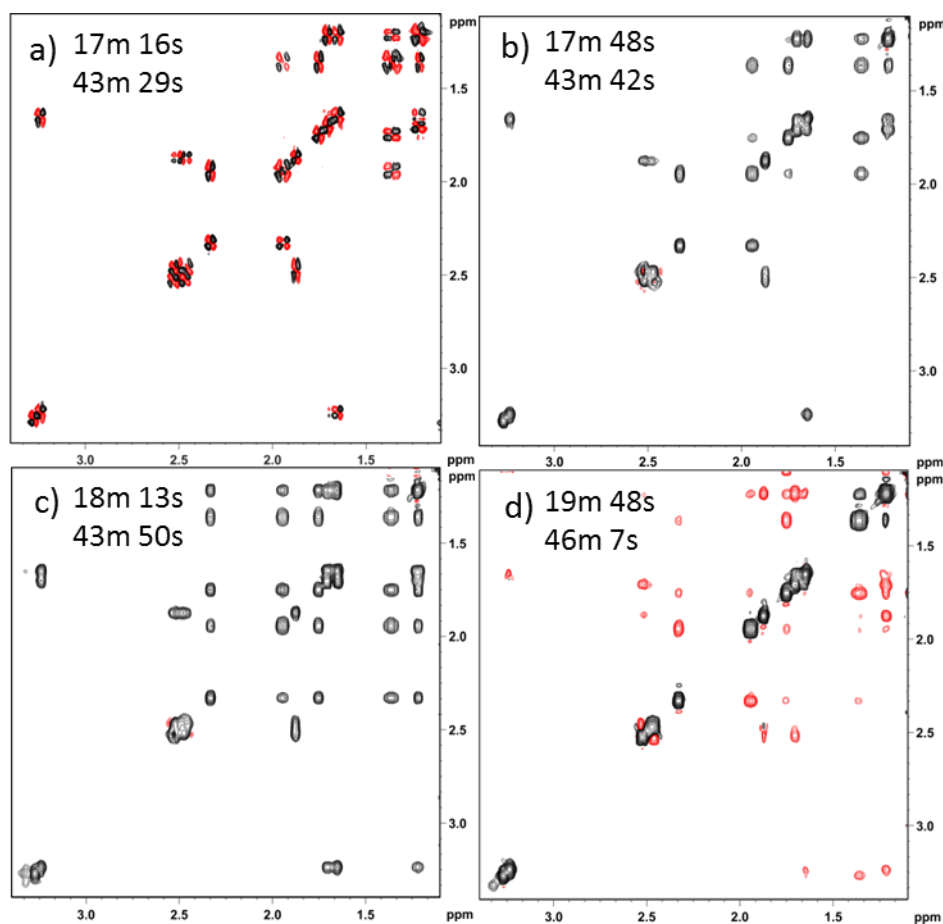


**Figure 3:** NOAH-3 BSX experiments performed on andrographolide showing expansions of the a) DQF-COSY, b) CLIP-COSY, c) TOCSY (80 ms mixing) and d) ROESY (300 ms mixing). Times given with each experiment compare those required for the NOAH-3 experiment (upper) with those for the combined duration of the three individual experiments (lower). Spectra were recorded on a room temperature TXI probe at 700 MHz (see Experimental section for full details).

When considering the utility of the NOAH experiments it is instructive to assess the sensitivity of each module's data that are collected. In all cases the requirements for adequate signal-to-noise are dictated by that of the least sensitive module in the sequence, and the BSX combinations are designed to optimise the sampling of magnetisation pools for each of these. The heteronuclear experiments are thus positioned early within each sequence, with the lower sensitivity HMBC the first to be acquired. Provided this experiment has adequate signal-to-noise ratio, the following modules will give good quality data. Relative to conventional experiments recorded with similar experimental parameters, we observe that the NOAH HMBC spectrum has typically >90%, the NOAH HSQC > 80% and the homonuclear modules have around 50% (ranging between 40-60%) of the signal intensity of the standalone versions (SI Fig S4). The homonuclear experiments exhibit the greatest intensity difference because they derive from longitudinal magnetisation that has recovered during the preceding modules, and despite this large relative attenuation, the absolute signal intensity is still far greater than that of the earlier modules which rely on sampling at  $^{13}\text{C}$  natural abundance, meaning this reduction is readily tolerated. As with most fast sampling schemes, NOAH will be optimum when detection sensitivity allows for a relatively small number of transients to be collected on each increment.

When detection sensitivity is sufficient, further time savings may be achieved through the use of non-uniform sampling (NUS)<sup>21</sup> which is compatible with the NOAH3 BSX experiments. Alternatively, increased resolution in the indirect dimensions may be afforded by such sampling, as previously explored.<sup>22</sup> Figure 4 compares the conventionally sampled *versus* NUS HSQC and HMBC data from BSC<sup>c</sup> experiments in which NUS was used to yield a four-fold resolution gain in the  $^{13}\text{C}$  dimension. This resolution enhancement is further exemplified by the summed carbon-13  $f_1$  projections from these data sets (Figure 5). These also appear to show the NUS peaks to stand more visibly above the baseline noise (although we resist comparing signal-to-noise ratios between conventional and NUS data sets due to the cosmetic de-noising imposed on reconstructed data<sup>21,22</sup>). A single python script is available to encode the necessary sampling into any parent NOAH experiment and prepare the necessary parameters (see supporting information). The NUS data sets are processed in the same manner (i.e. using the same processing scripts) as uniformly sampled NOAH data; see Experimental section.

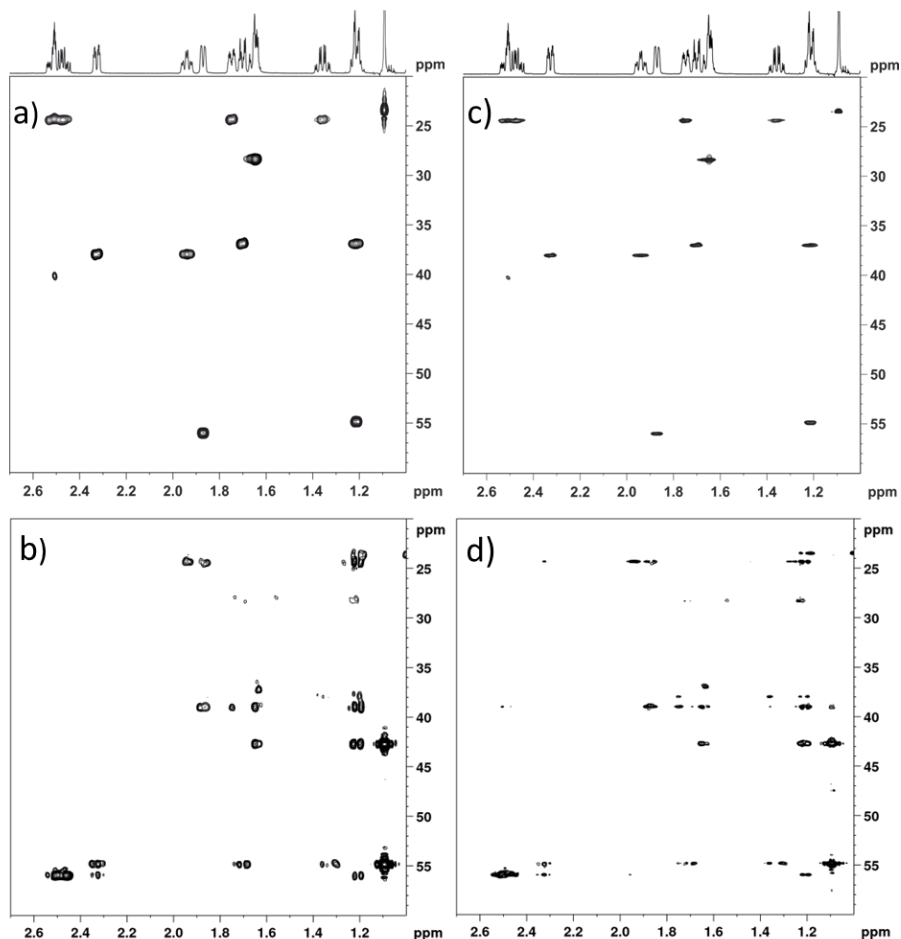


**Figure 4:** A comparison of spectra from NOAH-3 BSC<sup>c</sup> acquired using conventional sampling and that using non-uniform sampling for resolution enhancement. (a, b) HSQC and HMBC spectra collected with 256  $t_1$  points per module and (c,d) collected as 1024  $t_1$  points per module sampled non-uniformly at 25%; all other parameters were as described in the Experimental section. The experiment duration was 18 min for both NOAH experiments.

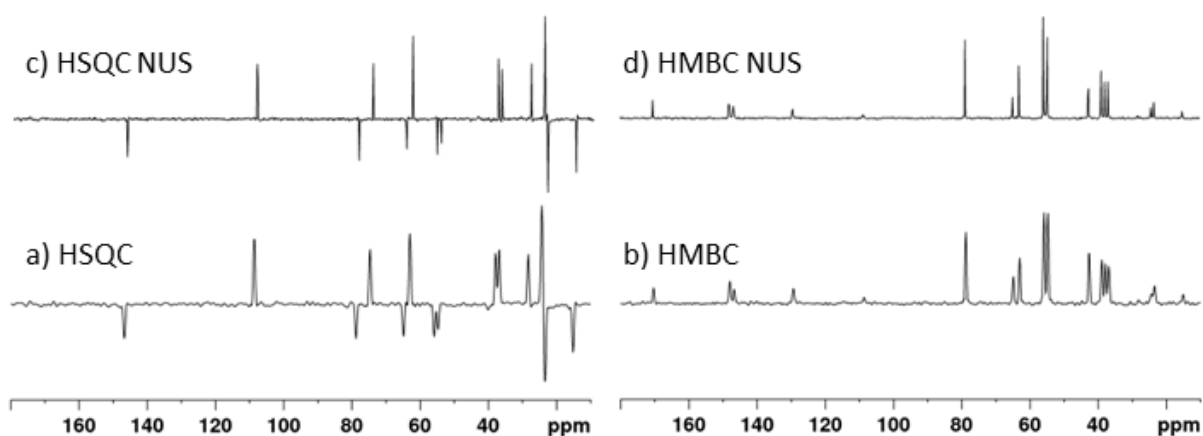


**Figure 5:** The summed  $^{13}\text{C } f_1$  projections from the NOAH-3 BSC<sup>c</sup> HSQC and HMBC data sets of Figure 4 illustrating the resolution gain achieved through NUS sampling of the NOAH modules.

In summary, the NOAH BSX sequences presented here offer the chemist a selection of module combinations of choice for routine structure characterisation of organic molecules. These provide for the most commonly employed 2D  $^1\text{H}$ - $^{13}\text{C}$  and  $^1\text{H}$ - $^1\text{H}$  correlation spectra and can be acquired on conventional two-channel instruments with no additional hardware

requirements. The experiments can be collected and processed directly from within automation, yielding individual 2D data sets. They are also compatible with NUS implementation, offering the potential for further time savings or for resolution enhancement when experimental conditions allow. These sequences should be well matched to the characterisation work flows of synthetic chemistry laboratories in particular, offering significant saving of valuable instrument time, simplifying the experiment setup and analysis.

## Experimental

Spectra were collected on a 38 mM andrographolide sample in DMSO recorded on either a room temperature triple-resonance TXI inverse probe at 700 MHz or a room temperature triple-resonance TBO broadband probe at 500 MHz on Bruker Avance III spectrometers running under TOPSPIN 3.5. Data were collected as 1K  $t_2$  data points with a 102 ms acquisition time using two transients for 256  $t_1$  increments per module and a recovery delay of 1.5 s. Delays were optimised for  $^1J_{CH} = 145$  Hz,  $^nJ_{CH} = 8$  Hz and  $J_{HH} = 30$  Hz for CLIP-COSY. TOCSY mixing (80 ms) used the DIPSI2 scheme with a 10 kHz  $B_1$  field, and the off-resonance ROESY employed two 150 ms spinlock pulses with WURST-40 amplitude profile<sup>23</sup> with a maximum  $B_1$  field of 5 kHz and offsets of +9.5 and -0.5 ppm (Fig 1f). Similar data were obtained through the use of repeated phase-alternating 180° pulses applied immediately after  $t_1''$  to provide the spin-lock (SI Fig S3). For this, the phase-alternating spin-lock sequence comprised 694 cycles of pairs of 216  $\mu$ s 180° pulses of opposite phase for a total 300 ms mixing period. Carbon 180° pulses were 0.5 ms CA WURST-20 adiabatic pulses with an 80 kHz sweep. In multiplicity editing, the J-compensated adiabatic pulses were 1.06 ms WURST-40 pulses with a 280 ppm sweep. All shaped adiabatic pulses were generated using the Bruker *Wavemaker* tool for optimum performance, although the sequences are compatible with Bruker's standard *prosol* settings. NOAH experiments employing NUS were set up within TOPSPIN with the *noah\_nus.py* python script.

Data sets were processed with zero-filling in  $f_2$  and linear prediction in  $f_1$  to 2K \* 1K points respectively. All NOAH data sets were processed within TOPSPIN with the *splitx\_au* program (defined by parameter *AUNMP*) to yield individual processed data sets for each NOAH module. The relevant processing parameters (including transform types and apodisation functions) for each separated experiment are defined by standalone AU scripts that are called directly by the *splitx\_au* routine; these AU scripts are defined in the NOAH parameters as the user-defined processing parameters *USERP1-USERP3*. For the BSX experiment family, these are named *noah\_hmbc*, *noah\_hsqc* and *noah\_xyz* respectively, where xyz is defined appropriately for the module X (e.g. *noah\_noesy* where X= NOESY). By default, all experiments are processed as echo-anti echo data, but this can be modified through the use of appropriate arguments with the *USERP3* setting for the homonuclear module; for example *USERP3=noah\_noesy States* to define the required States based processing of the NOESY data. All scripts are available from the authors and are provided as supporting files.

## References

1. Ě. Kupče, and T. D. W. Claridge, *Angew. Chem. Int. Ed.*, 2017, **56**, 11779-11783.
2. Ě. Kupče, and T. D. W. Claridge, *Chem. Commun.*, 2018, **54**, 7139-7142.
3. P. Nolis, M. Pérez-Trujillo, and T. Parella, *Angew. Chem. Int. Ed.*, 2007, **46**, 7495-7497.



4. K. Motiram-Corral, M. Pérez-Trujillo, P. Nolis, and T. Parella, *Chem. Commun.*, 2018, **54**, 13507-13510.
5. P. Nolis, and T. Parella, *Magn. Reson. Chem.*, 2019, **57**, 85-94.
6. P. Nolis, K. Motiram-Corral, M. Pérez-Trujillo, and T. Parella, *ChemPhysChem*, 2019, **20**, 356-360.
7. Ě. Kupče, R. Freeman, and B. K. John, *J. Am. Chem. Soc.*, 2006, **128**, 9606-9607.
8. Ě. Kupče, in *Modern NMR Methodology*, eds. H. Heise and S. Matthews, Springer, Berlin, 2013, pp. 71-96.
9. H. Kovacs, and Ě. Kupče, *Magn. Reson. Chem.*, 2016, **54**, 544-560.
10. M. Mishkovsky, and L. Frydman, *Ann. Rev. Phys. Chem.*, 2009, **60**, 429-448.
11. A. Tal, and L. Frydman, *Prog. Nucl. Magn. Reson. Spectrosc.*, 2010, **57**, 241-292.
12. M. Gal, and L. Frydman, *Magn. Reson. Chem.*, 2015, **53**, 971-985.
13. Ě. Kupče, and R. Freeman, *Magn. Reson. Chem.*, 2007, **45**, 2-4.
14. D. Schulze-Sünninghausen, J. Becker, and B. Luy, *J. Am. Chem. Soc.*, 2014, **136**, 1242-1245.
15. M. R. M. Koos, G. Kummerlöwe, L. Kaltschnee, C. M. Thiele, and B. Luy, *Angew. Chem. Int. Ed.*, 2016, **55**, 7655-7659.
16. Ě. Kupče, and R. Freeman, *J. Magn. Reson.*, 1997, **127**, 36-48.
17. C. Zwahlen, P. Legault, S. J. F. Vincent, J. Greenblatt, R. Konrat, and L. E. Kay, *J. Am. Chem. Soc.*, 1997, **119**, 6711-6721.
18. M. J. Thrippleton, and J. Keeler, *Angew. Chem. Int. Ed.*, 2003, **42**, 3938-3941.
19. Christina M. Thiele, K. Petzold, and J. Schleucher, *Chem. Eur. J.*, 2009, **15**, 585-588.
20. T. L. Hwang, and A. J. Shaka, *J. Am. Chem. Soc.*, 1992, **114**, 3157-3159.
21. K. Kazimierczuk, and V. Orekhov, *Magn. Reson. Chem.*, 2015, **53**, 921-926.
22. A. Le Guennec, J.-N. Dumez, P. Giraudeau, and S. Caldarelli, *Magn. Reson. Chem.*, 2015, **53**, 913-920.
23. Ě. Kupče, and R. Freeman, *J. Magn. Reson.*, 1995, **115A**, 273-276.

Experiment	Module X In BSX	NOAH duration	Summed duration	NOAH vs summed
NOAH-3 BSC	COSY	17m 21s	43m 8s	0.40
NOAH-3 BSC <sup>c</sup>	CLIP-COSY	17m 48s	43m 42s	0.41
NOAH-3 BSD	DQF-COSY	17m 16s	43m 29s	0.40
NOAH-3 BST	TOCSY (80 ms)	18m 13s	43m 50s	0.42
NOAH-3 BSN	NOESY (400 ms)	20m 40s	46m 19s	0.45
NOAH-3 BSR	ROESY (300 ms)	19m 48s	46m 7s	0.43

**Table 1:** Comparison of experiment times of NOAH-3 experiments versus parent experiments. Summed durations show the total time requirements of the three corresponding individual experiments recorded with identical resolution (see SI Table S1 for full timing details).